

# Formation of Optical Solitons in Nonlinear Photonic Crystal Waveguides \*

LAN Sheng(兰胜)\*\*, CHEN Xiong-Wen(陈雄文)

*Department of Physics, Shantou University, Shantou 515063*

(Received 18 March 2004)

*Relying on the huge group velocity dispersion available in photonic crystal (PC) waveguides, we observe the formation of both Bragg grating solitons and gap solitons in nonlinear PC waveguides in numerical experiments. Also, we indicate the potential applications of optical solitons in optical limiting, optical delay, and pulse compression and the feasibility of observing optical solitons in practical experiments.*

PACS: 42.70.Qs, 42.65.Tg, 42.65.Wi

Solitons in optical fibres were first suggested by Hasegawa and Tappert in 1973.<sup>[1]</sup> Physically, they originate from the balance between the dispersion and nonlinearity of the materials (or structures).<sup>[2]</sup> To date, solitons have been studied in various nonlinear bulk<sup>[3]</sup> and periodic structures, including Bragg gratings,<sup>[4–6]</sup> Bragg stacks,<sup>[7]</sup> waveguide arrays,<sup>[8]</sup> and photonic crystals (PCs).<sup>[9–11]</sup> At present, two-dimensional (2D) PC slabs instead of real three-dimensional (3D) PCs are widely used as a platform to manipulate the flow of light because they are easy to be fabricated and integrated with other devices. The most popular PC structure is generally formed by patterning a triangular lattice of air holes in a high-index dielectric material (e.g., a semiconductor such as GaAs or Si).<sup>[12]</sup> As compared with the Bragg gratings and stacks, due to the strong periodic modulation in refractive index, 2D PC slabs are expected to exhibit much wider gaps and particularly much larger group velocity dispersion (GVD). Similarly, we can anticipate very large GVD at the edge of the impurity band corresponding to a line-defect waveguide formed in 2D PC slabs. The linear properties of line-defect waveguides have been investigated in detail both theoretically and experimentally because of their importance in building PC-based devices and PC integrated circuits.<sup>[13]</sup> However, their nonlinear properties and corresponding applications remain unexplored. In principle, it is possible to generate optical solitons in nonlinear PC waveguides. The huge GVD of the nonlinear PC waveguides has two implications. To observe optical solitons, firstly much higher power density will be needed, and secondly the total length of the nonlinear PC waveguide needed will be dramatically reduced.<sup>[2]</sup> The latter feature offers us an opportunity to observe the formation of optical solitons and to investigate their properties and applications by numerical simulation. Otherwise, it would be very difficult to simulate the generation of optical solitons in

nonlinear PC waveguides based on the current computational resource. In addition, although the demonstration of an enhancement in nonlinearity accompanied with the huge GVD is still lacking, it is expected to partly relax the requirement for increased power density, making it possible to observe optical solitons in practical experiments.

In this Letter, we demonstrate the formation of optical solitons in nonlinear PC waveguides by numerical simulation. Based on this, we indicate that optical solitons can be experimentally observed under very reasonable excitation conditions.

A schematic of the nonlinear PC waveguide, a line-defect waveguide in a 2D PC (a triangular lattice of air holes in GaAs), is shown in Fig. 1(a). The radius of the air holes is chosen to be  $0.3a$ , where  $a = 0.4 \mu\text{m}$  is the lattice constant. Considering a reasonable simulation speed with the available computation resource, we have chosen to simulate a pure 2D PC structure with an effective refractive index of  $\sim 2.87$  using nonlinear finite-difference time-domain (FDTD) method.<sup>[14]</sup> This approximation has been confirmed to be effective for 2D PC slabs.<sup>[15]</sup> The effective refractive index for PC slabs depends mainly on the thickness of slabs and the radius of air holes. However, the change in effective refractive index leads only to a shift of the frequency spectra and does not affect the main conclusions drawn in this study. A perfectly matched layer boundary condition is employed for the FDTD simulation.<sup>[16]</sup> The grid sizes used in the simulation are  $a/10$  and  $\sqrt{3}a/10$ , respectively, for the directions parallel and perpendicular to the waveguide. A further reduction in the grid size barely influences the simulation results. Two slab waveguides of width  $\sqrt{3}a$  are used to couple light into and out of the PC waveguide. Also, the coupling efficiency is found to be maximum for a direct coupling [i.e.  $d = 0$  in Fig. 1(a)]. For comparison, a slab waveguide of width  $\sqrt{3}a$  is used as a reference, as shown in Fig. 1(b).

\* Supported by the National Natural Science Foundation of China under Grant No 10374065, the Natural Science Foundation of Guangdong Province (No 32050), and the Department of Education of Guangdong Province (Z03033).

\*\* Email: slan@stu.edu.cn

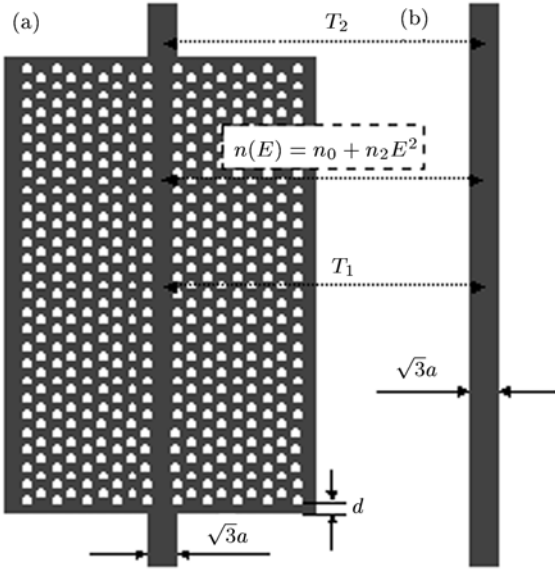


**Fig. 1.** Schematic of the nonlinear PC waveguide considered in this paper (a) and the slab waveguide used as a reference (b). The actual total length of the PC waveguide is  $42a$ .

The dispersion curves for the line-defect waveguide can be obtained by either plane wave expansion or FDTD methods. The calculated dispersion curves for transverse magnetic (TM, electric field lies in the 2D plane) mode are shown in Fig. 2(a). In general, the odd mode will not be excited in the case of normal incidence. Here we focus on the low-energy band edge of the even mode where very large GVD exists. The transmission spectrum obtained by numerical simulation using a continuous wave source is given in Fig. 2(b).

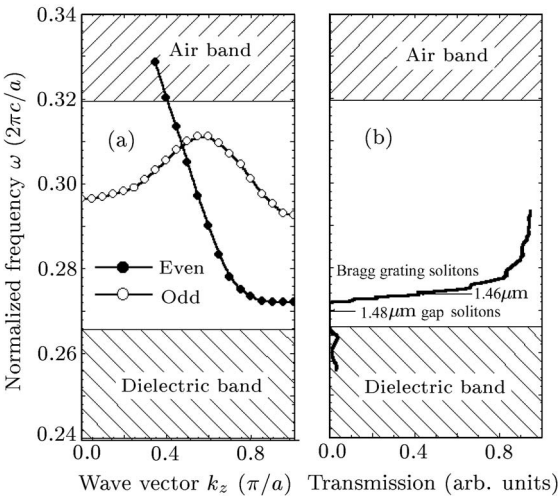


**Fig. 2.** (a) Calculated dispersion curves for the TM mode of the PC waveguide. (b) Simulated transmission spectrum for the PC waveguide by using a continuous wave source. The low transmission detected in the dielectric band is due to the leakage of light from the line-defect waveguide into the surrounding PC.

With the dispersive curve, the group velocity  $v_g$  and the GVD ( $\beta_2$ ) near the band edge can be readily derived. It is remarkable that  $\beta_2$  is extremely large (in the order of  $10^7$  ps<sup>2</sup>/m) at the band edge ( $\omega = 0.2721$  ( $2\pi c/a$ ) or  $\lambda = 1.47 \mu\text{m}$ , where  $\omega$  and  $\lambda$  represent the normalized frequency and wavelength respectively). This value is three orders of magnitude larger than that in Bragg gratings.<sup>[5]</sup> Even at  $1.46 \mu\text{m}$  (or  $\omega = 0.2740$  ( $2\pi c/a$ )), which is 10 nm from the band edge,  $\beta_2$  is still six orders of magnitude larger than that in conventional optical fibres.<sup>[2]</sup>

Assuming that the PC waveguide is made of a Kerr nonlinear material, then the nonlinear refractive index change  $\Delta n$  is proportional to the local electric field intensity ( $|E|^2$ ), i.e.

$$\Delta n = n_2 |E|^2, \quad (1)$$

where  $n_2$  is the nonlinear coefficient of the material. For GaAs and  $\text{Al}_x\text{Ga}_{1-x}\text{As}$ , their nonlinear properties near the half-gap energies are well described by Eq. (1). Also, it should be pointed out that their  $n_2$  is about 500 times larger than silica used for making optical fibres.<sup>[17]</sup>

Very similar to that in optical fibres, we can describe the effects of GVD and SPM (self-phase modulation) in the nonlinear PC waveguide with two length scales which are generally referred to as dispersion length  $L_D$  and nonlinear length  $L_{NL}$ .<sup>[2]</sup> They are defined as follows:

$$L_D = \frac{T_0^2}{|\beta_2|}, \quad (2)$$

$$L_{NL} = \left( \frac{2\pi}{\lambda_0} n_2^{\text{eff}} P_{\text{eff}} \right)^{-1}. \quad (3)$$

In Eq. (2),  $T_0$  is the half width of the input pulse at 1/e-intensity point. In Eq. (3),  $\lambda_0$  is the wavelength of the input pulse in vacuum,  $n_2^{\text{eff}} = \alpha n_2$  represents the effective nonlinear coefficient and  $\alpha$  is the so-called enhancement factor;  $P_{\text{eff}} = \eta P_0$  denotes the effective power density at the peak of the input pulse,  $P_0$  is the peak power density of the input pulse, and  $\eta$  is the coupling efficiency.

In general, the interplay of GVD and SPM effects gives rise to optical solitons of order  $\tilde{N}$ , with  $\tilde{N}$  determined by

$$\tilde{N} = \left( \frac{L_D}{L_{NL}} \right)^{1/2} + \varepsilon, \quad (4)$$

where  $\tilde{N}$  is an integer and  $|\varepsilon| < 0.5$ . With respect to the initial pulse, the width of the generated solitons is narrowed for a positive  $\varepsilon$  and broadened for a negative  $\varepsilon$ .

Let us consider a subpicosecond pulse at  $1.46 \mu\text{m}$  where  $|\beta_2| \approx 10^4$  ps<sup>2</sup>/m. If  $T_{\text{FWHM}} = 1.665 T_0 = 0.3$  ps, then  $L_D \approx 8.4 \mu\text{m}$ . In order to satisfy the basic condition for the formation of solitons ( $L > L_D \geq$

$L_{NL}$ ), the total length of the nonlinear PC waveguide  $L$  is chosen to be  $2L_D \approx 16.8 \mu\text{m} = 42a$ . Then we fix  $n_2$  at  $1 \times 10^{-5} \mu\text{m}^2/\text{W}$  (or  $1 \times 10^{-13} \text{cm}^2/\text{W}$ ) and adjust  $P_0$ , and correspondingly  $L_{NL}$ , to see the formation of Bragg grating solitons in the numerical simulation.

The simulation results are shown in Fig. 3. For a very weak  $P_0$  ( $P_0 = 1 \text{W}/\mu\text{m}^2$ ), we can clearly see the continuous broadening of the pulse width which is recorded by two monitors placed in the middle of the waveguide and in the output slab waveguide. The recorded pulse intensities are denoted as  $T_1$  and  $T_2$  respectively. Also, it is noted that the broadening is asymmetric because  $\beta_2$  is a highly nonlinear function of wavelength near the band edge. A broadening factor of  $\sim 1.5$  observed in the middle of the waveguide indicates that  $L_D$  is about  $8.4 \mu\text{m}$ .<sup>[2]</sup> This value is in good agreement with that estimated by Eq. (2). By increasing  $P_0$  to  $3 \times 10^2 \text{W}/\mu\text{m}^2$ , however, no pulse broadening is observed. Instead, a symmetric pulse shape with a slightly narrower width is achieved and it propagates along the waveguide without any change. This feature clearly indicates the formation of optical solitons.<sup>[2]</sup> The fact that the generated soliton is of identical width to the input pulse suggests that  $\varepsilon$  is close to 0 under this excitation condition. A further increase of  $P_0$  to  $6 \times 10^2 \text{W}/\mu\text{m}^2$  leads to a significant narrowing of pulse width and an obvious change in the pulse shape, confirming again the generation of solitons.<sup>[2]</sup> A careful inspection reveals that the integrated intensity of the soliton is enhanced while its group velocity is increased with increasing  $P_0$ .

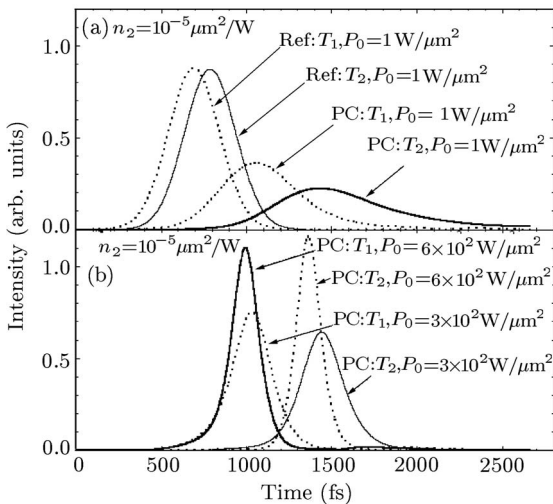


**Fig. 3.** Evolution of the transmitted pulses through the nonlinear PC waveguide with increasing power density  $P_0$  for the input pulse. The pulse intensities recorded in the middle of the waveguide and in the output waveguide are denoted as  $T_1$  and  $T_2$  respectively. The pulse shape in the reference waveguide is also provided for comparison.

With the knowledge of  $P_0$  ( $\sim 3 \times 10^2 \text{W}/\mu\text{m}^2$ ) em-

ployed to generate the fundamental solitons, it is possible to extract the nonlinearity enhancement factor  $\alpha$ . In our case, it is actually the ratio of the nonlinear phase shift achieved in the PC waveguide to that obtained in the reference waveguide. For fundamental solitons whose width is similar to that of the input pulse, we have  $\varepsilon \approx 0$  and  $L_{NL} \approx L_D$ . Thus, the enhancement factor can be easily derived from the definition of  $L_{NL}$  [Eq. (3)]. For  $\lambda_0 = 1.46 \mu\text{m}$ ,  $n_2 = 1 \times 10^{-5} \text{W}/\mu\text{m}^2$ ,  $\eta \approx 0.87$ ,  $P_0 \approx 3 \times 10^2 \text{W}/\mu\text{m}^2$ , we obtain  $\alpha \approx 10.6$  indicating that we do achieve an enhancement of nonlinearity in the PC waveguide.

Now let us see the formation and characteristics of gap solitons in the nonlinear PC waveguide. We set the input pulse at  $1.48 \mu\text{m}$  (or  $\omega = 0.2703(2\pi c/a)$ ) and for a fixed  $n_2$  of  $1 \times 10^{-5} \mu\text{m}^2/\text{W}$  increased the input power to see the formation of gap solitons. The simulation results for a 0.3-ps pulse are presented in Fig. 4. For power densities weaker than  $10^3 \text{W}/\mu\text{m}^2$ , the pulse is totally blocked by the band gap. Raising the power density to  $2 \times 10^3 \text{W}/\mu\text{m}^2$ , we can see a transmitted pulse with markedly narrowed pulse width. Further increase of the power density results in narrower pulse width, larger group velocity and enhanced transmittance. These phenomena imply that nonlinear PC waveguides with large GVD can be employed as nice optical limiters, efficient pulse compressors and controllable optical delay lines. These applications will be discussed in detail elsewhere.

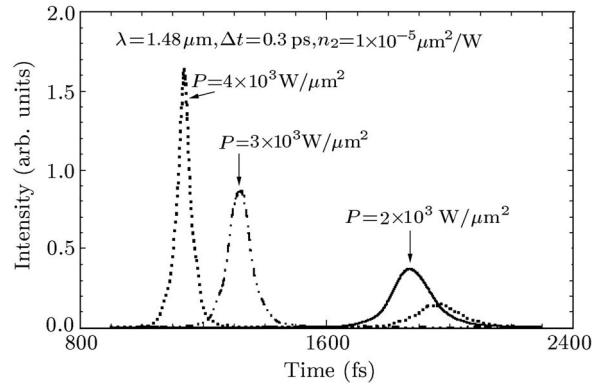


**Fig. 4.** Formation of gap solitons with increasing power density for the input pulse.

Let us check the feasibility of optical solitons in practical nonlinear PC waveguides. The nonlinear coefficient we used in the simulation is very close to the practical values for GaAs and AlGaAs ( $\sim 2 \times 10^{-13} \text{cm}^2/\text{W}$ ).<sup>[17]</sup> The power densities necessary to observe the formation of optical solitons are  $3 \times 10^2 \text{W}/\mu\text{m}^2$  (or  $30 \text{GW}/\text{cm}^2$ ) and  $2 \times 10^3 \text{W}/\mu\text{m}^2$  (or  $200 \text{GW}/\text{cm}^2$ ) for Bragg grating solitons and gap solitons respectively. Previously, similar power density ( $10 \text{GW}/\text{cm}^2$ ) has been used to observe spatial solitons in waveguide arrays.<sup>[8]</sup> A further reduction of

the required power density can be achieved by increasing the pulse width as well as the waveguide length. For instance, the required power density can be reduced by two orders of magnitude if we use 1-ps pulse and increase the waveguide length to 168  $\mu\text{m}$ . Therefore, optical solitons can be observed in practical PC waveguides under very reasonable excitation conditions.

In summary, we have investigated the formation and characteristics of optical solitons in nonlinear PC waveguides. It is shown that both Bragg grating solitons and gap solitons can be generated in nonlinear PC waveguides under very reasonable excitation conditions. They exhibit potential applications such as optical limiting, pulse compression and optical delay.

## References

- [1] Hasegawa A and Tappert F 1973 *Appl. Phys. Lett.* **23** 142
- [2] Agrawal G P 1995 *Nonlinear Fiber Optics: Second Edition* eds Liao P F, Kelley P L and Kaminow I (San Diego, CA: Academic) chap 5
- [3] Cui W N, Sun C L and Huang G X 2003 *Chin. Phys. Lett.* **20** 246
- [4] Christodoulides D N and Joseph R I 1989 *Phys. Rev. Lett.* **62** 1746
- [5] Eggleton B J, Slusher R E, Sterke C M de, Krug P A and Sipe J E 1996 *Phys. Rev. Lett.* **76** 1627
- [6] Eggleton B J, Sterke C M de and Slusher R E 1997 *J. Opt. Soc. Am. B* **14** 2980
- [7] Chen W and Mills D L 1987 *Phys. Rev. Lett.* **58** 160
- [8] Eisenberg H S, Silberberg Y, Morandotti R, Boyd A R and Aitchison J S 1998 *Phys. Rev. Lett.* **81** 3383
- [9] John S and Aközbeke N 1993 *Phys. Rev. Lett.* **71** 1168
- [10] Mingaleev S F and Kivshar Y S 2001 *Phys. Rev. Lett.* **86** 5474
- [11] Christodoulides D N and Efremidis N K 2002 *Opt. Lett.* **27** 568
- [12] See for example, Kawai N, Inoue K, Carlsson N, Ikeda N, Sugimoto Y, Asakawa K and Takemori T 2001 *Phys. Rev. Lett.* **86** 2289
- [13] Notomi M, Yamada K, Shinya A, Takahashi J, Takahashi C and Yokohama I 2001 *Phys. Rev. Lett.* **87** 253902
- [14] Yee K S 1966 *IEEE Trans. Antennas Propag.* **AP-14** 302. In this article, a commercially available software developed by Rsoft Design Group (<http://www.rsoftdesign.com>) is used for nonlinear FDTD simulation.
- [15] Qiu M 2002 *Appl. Phys. Lett.* **81** 1163
- [16] Berenger J P 1994 *J. Comput. Phys.* **114** 185
- [17] Aitchison J S, Hutchings D C, Kang J U, Stegeman G I and Villeneuve A 1997 *IEEE J. Quantum Electron.* **33** 341